

Arild Lohne, Arne Stavland, Siv M. Åsen,  
Olav Aursjø and Aksel Hiorth



## Recommended polymer workflow

Interpretation and parameter identification

REPORT NO. 114, UNIVERSITY OF STAVANGER  
30th NOVEMBER 2021

The National  
IOR Centre  
of Norway



## Reports from UiS

### Recommended polymer workflow - Interpretation and parameter identification

Arild Lohne<sup>1</sup>, Arne Stavland<sup>1</sup>, Siv M. Åsen<sup>1</sup>, Olav Aursjø<sup>1</sup>, and Aksel Hiorth<sup>2,1</sup>

Rapport no.	114
Publisher	University of Stavanger
	<a href="http://www.uis.no">www.uis.no</a>
Project title	The National IOR Centre
ISBN	978-82-8439-098-7
ISSN (online)	2387-6662
ISSN (print)	0806-7031
DOI	<a href="https://doi.org/10.31265/usps.202">https://doi.org/10.31265/usps.202</a>

Lisens: [CC BY 4.0](https://creativecommons.org/licenses/by/4.0/)



---

<sup>1</sup> NORCE Research, Norway

<sup>2</sup> University of Stavanger, Norway

# Recommended polymer workflow—

Interpretation and parameter identification



Arild Lohne, Arne Stavland, Siv M. Åsen,  
Olav Aursjø (NORCE) and Aksel Hiorth (UiS)  
30th November 2021

## **Acknowledgement**

The authors of recommended practices acknowledge the Research Council of Norway and the industry partners, ConocoPhillips Skandinavia AS, Aker BP ASA, Vår Energi AS, Equinor Energy AS, Neptune Energy Norge AS, Lundin Energy Norway AS, Halliburton AS, Schlumberger Norge AS, and Wintershall Dea Norge AS, of The National IOR Centre of Norway for support.



Contents

Objective and target audience ..... 2

    Summary ..... 2

Introduction ..... 2

    Data and Physics driven approach ..... 3

Methodological Approach ..... 3

    Experimental input..... 3

    Bulk viscosity ..... 4

    Flow in porous medium..... 9

        Single phase core experiments..... 11

        Adsorption and permeability reduction .....14

        Two-phase experiments .....15

    Recommended workflow .....15

Validation .....16

Conclusions and recommendations .....16

    Knowledge Gaps .....17

References .....17

## Objective and target audience

Main objectives: give an overview of important mechanisms in polymer flooding and how these mechanisms are represented in IORCoreSim, and describe necessary laboratory input to determine model parameters which can be used for scale-independent predictions of polymer behavior. A high-level illustration of the workflow is given in Figure 1.

This report is addressing people with an interest in polymer modelling and/or simulation of polymer flooding.

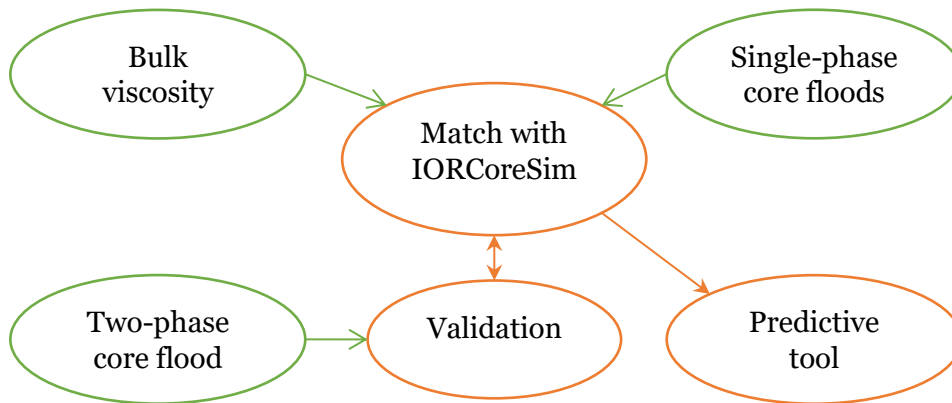


Figure 1 Schematic illustration on how IORCoreSim can be used for predictive simulations of polymer flooding.

## Summary

Injecting a polymer solution into a porous medium significantly increases the modeling complexity, compared to model a polymer bulk solution. Even if the polymer solution is injected at a constant rate into the porous medium, the polymers experience different flow regimes in each pore and pore throat. The main challenge is to assign a macroscopic porous media “viscosity” to the fluid which can be used in Darcy law to get the correct relationship between the injection rate and pressure drop. One can achieve this by simply tabulating experimental results (e.g., injection rate vs pressure drop). The challenge with the tabulated approach is that it requires a huge experimental database to tabulate all kind of possible situations that might occur in a reservoir (e.g., changing temperature, salinity, flooding history, permeability, porosity, wettability etc.). The approach presented in this report is to model the mechanisms and describe them in terms of mathematical models. The mathematical model contains a limited number of parameters that needs to be determined experimentally. Once these parameters are determined, there is in principle no need to perform additional experiments.

## Introduction

Polymer is mainly a method for reducing the water production by reducing the water mobility. The immediate effect of polymer injection on the oil production rate depends on to what extent the oil pressure gradient towards the production wells can be maintained and on changes in flow pattern in a multi-well area. The critical issue in this period is most likely polymer injectivity. Later, when polymer have reached deeper into the reservoir, linear displacement efficiency, areal and vertical sweep effects become more important.

In this document we focus on how to make reliable prediction of polymer behavior at the field scale based on information obtained from laboratory experiments. To Interpret experiments

we have developed a set of mathematical models consistent with the underlying (pore scale) physics and experimental observations. We describe here the interpretation with IORCoreSim (the models), important model parameters and experimental input needed.

Polymer models available in commercial simulators are in general too simple to effectively handle all field scale variations of properties such as permeability, temperature, saturation and flow rate. A particular problem with synthetic polymer is to predict injectivity if shear thickening and mechanical degradation occurs, and then to include effects of eventual degradation on the polymer properties beyond the near-well shear thickening zone. Much can be resolved by using different model parameters in different parts of the field model, but there might be significant uncertainty in what these parameters should be and in the final simulated effect of polymer.

### Data and Physics driven approach

An important principle in the polymer modeling in IORCoreSim [1, 2] has been to include most, if not all, important dependencies through physical models to achieve model parameters independent of varying conditions. In the end, we want models to predict a relationship between pressure gradient and flow rate. Apparently, this relation could be measured experimentally and represented in form of a table (data driven). However, this table is only fully valid for the conditions under which it was measured. One solution could be to repeat the measurement and create a lot of tables covering all dependencies, and then interpolate between them. This approach is expensive and time consuming, a much better approach is to utilize known physical relations and use appropriate mathematical expressions (physics driven). For non-linear relations, and if the number of dependencies is high, this method will require much less experimental input. A similar approach is used in ref. [3].

The above-mentioned relation between pressure gradient and flow rate depends on the polymer solution viscosity, which again is a function of polymer properties, concentration, temperature, and in-situ shear rate, and on core properties like permeability, porosity and saturation. Identified mechanisms; the effect of a polymer depleted layer at the rock surface, the onset of elongational flow (“shear thickening”) and mechanical degradation at high flow rates, do all depend on both rock and polymer properties.

The polymer models in IORCoreSim handle the effect of polymer concentration, temperature and salinity and the in-situ rheological behavior of polymer at varying permeability and porosity, and at different flow regimes. The problem with a well penetrating a large grid block is solved by a radial numerical integration of rheological behavior for the well block. The models calibrated against laboratory data can next be used for predicting polymer behavior in well blocks and different geological zones, and to investigate sweep effects in small large-scale models, but the tool (IORCoreSim) is not capable for solving the full field scale flow pattern. A possible workflow might be to use IORCoreSim to generate appropriate input parameters for different zones which can be used in a commercial simulator.

### Methodological Approach

The description in this document is limited to regular polymers with a non-associative behavior. A description of available options for associative polymers can be found in the IORCoreSim manual and in [4]. Polymer parameter set used in this report is available from the IORCoreSim\Cases\Polymer directory at IORCentre Teams in the document *HPAM\_SW\_polymerdata.txt* and in subdirectory *hp1530\_coreflood*.

### Experimental input

To make reliable simulations of polymer flow in porous medium, the polymer model must be tuned to experimental data. That is, all the model parameters in the different sub-models must

be determined by matching appropriate experimental data. The main parts of the polymer model are:

- Bulk viscosity model representing the Newtonian and shear thinning regimes.
- Expression for in-situ shear rate.
- Adsorption model.
- Permeability reduction model computing *RRF* (*Residual resistance factor*) as function of adsorption and polymer properties.
- Depletion layer model computing an apparent viscosity from bulk viscosity and the depletion layer thickness.
- Elongation model capturing the shear thickening behavior observed with synthetic polymers.
- Shear degradation model.

If one wants to evaluate a new polymer, one must obviously measure the bulk viscosity and determine the parameters in the bulk viscosity model. The parameters for the remaining models are obtained from core experiments.

Once tuned and validated against a basis set of experimental data, the model can be used independent of experiments to predict polymer behavior within the variable space covered by the base set. New experimental data can be used to improve the model (fine tuning) or expand the variable space. The mentioned data set for HPAM was obtained at room temperature and with 1500 ppm polymer dissolved in synthetic sea water for all the core experiments except one where 600 ppm was used. If one wants to use the model at higher concentrations or with reduced salinity or at a different temperature, additional core flood experiments would be needed for validation and re-tuning of model parameters. Note that the number of experiments is still limited compared to using a pure data driven approach with tables.

In Ref. [1] a series of single-phase experiments [2] using hydrolysed polyacrylamide (HPAM) with molecular weight ranging from 5 to 20 MDalton and permeability ranging from 160 mD to 2000 mD were matched using a single set of model parameters for the in-situ behavior of polymer (listed in Input 3). The polymer model (i.e., the parameter set) was later reused in a study of associative polymer [4] which also included two-phase experiments.

The experimental input needed are from experiments of type:

- Bulk viscosity
- Single phase core experiments
- 2-phase core experiments

The bulk viscosity data is the bases for doing any evaluation of a polymer. Single-phase core experiments in combination with the bulk viscosity will contain information about in-situ rheology and adsorption/*RRF* and can be used for validation and/or parameter tuning. The presence of oil is essentially modeled by replacing porosity  $\phi$  with  $\phi \cdot S_w$  and absolute permeability  $k$  with  $k_w = k \cdot k_{rw}$  in appropriate expressions, while polymer model parameters are assumingly not affected. It is therefore recommended to determine all polymer parameters related to in-situ flow from single-phase experiments to avoid complicating the interpretation with  $k_w$  and  $\phi \cdot S_w$  changing during the measurements. Finally, the model should be tested against two-phase experiments for final validation. For making field scale predictions, polymer adsorption and *RRF* should be measured on reservoir core under representative wettability conditions.

### Bulk viscosity

Bulk viscosity of polymer solutions is typically measured in a rheometer covering a shear rate ( $\dot{\gamma}$ ) ranging from below 1 to above 100  $s^{-1}$ . An example of such measurement given in Figure 1 demonstrates two shear rate regimes, a flat plateau at low shear rate with constant viscosity

(Newtonian behavior) and a shear thinning regime at higher shear rate. If plotted as specific viscosity ( $\eta_{sp}$ , see Eq. 7) versus shear rate on a log-log plot, the data in the shear thinning part should fit a straight line with a negative slope  $-n$  referred to as the shear thinning index for that polymer solution. The intersection between the shear thinning line and the Newtonian plateau gives the polymer relaxation time  $\lambda_1$  (inverse value of corresponding shear rate  $\dot{\gamma}$ ).

All the equations used in calculating the bulk viscosity in IORCoreSim are listed in Table 1 and all required input parameters are listed in Table 2. The parameters that must be determined from laboratory measurements are in dark red color, while the initial molecular weight ( $M_{w0}$ ) would normally be obtained from vendors. The Mark Houwink exponent  $\alpha_{Mw}$  will only have an effect on computed bulk viscosity if polymer  $M_w$  is reduced by degradation, and any value in the range 0.6 to 1 should be fine.

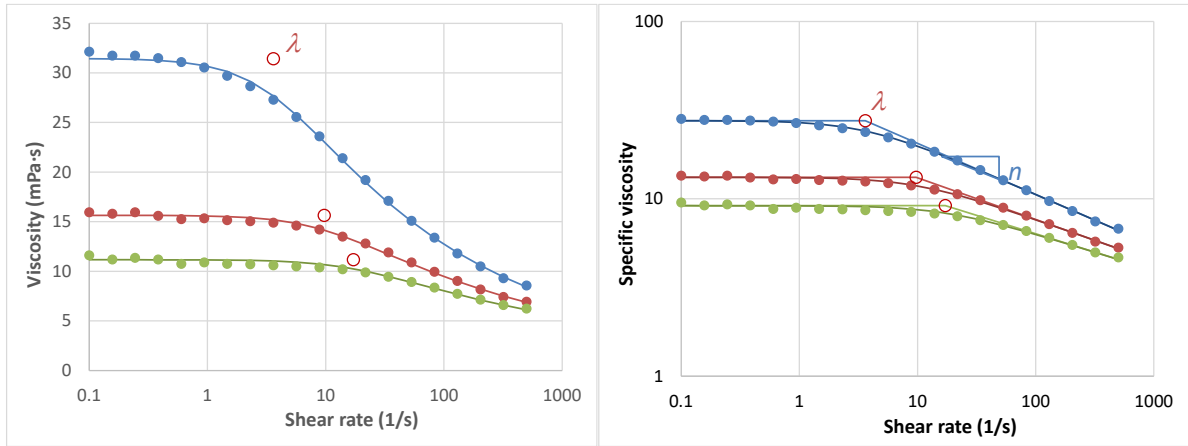


Figure 1 Viscosity measured for 2000 ppm polymer solutions with different molecular weights. Left: solution viscosity (linear scale) and right: specific viscosity (log-scale). Experimental data are fitted with the Carreau model (lines).

Table 1: Bulk viscosity equations in IORCoreSim. Red symbols need to be measured, and the orange parameters are from literature or manufactory.

Intrinsic viscosity $[\eta]$ dependence on changes in $M_w$ and temperature:	$[\eta] = [\eta]_0 \left( \frac{M_w}{M_{w0}} \right)^{\alpha_{Mw}} \left( 1 - B_{pT}(T - T_0) \right),$	(1)
Specific viscosity at zero shear rate, Alternative 1, third order polynomial:	$\eta_{sp0} = c_p[\eta] + k'(c_p[\eta])^2 + k''(c_p[\eta])^3$	(2a)
Alternative 2, Martin Eq.:	$\eta_{sp0} = c_p[\eta] \cdot e^{c_p[\eta]k'}$	(2b)
Shear thinning, specific viscosity $\eta_{sp}$ :	$\eta_{sp} = \frac{\eta_{sp0}}{(1 + (\lambda_1 \dot{\gamma})^{x_1})^{n_1/x_1}},$	(3)
Shear thinning index $n$ :	$n = 1 - \frac{1}{1 + (a_n[\eta]c_p)^{b_n}}$	(4)
Relaxation parameter $\lambda_1$ :	$\lambda_1 = \lambda_a \cdot \frac{\eta_s \eta_{sp0} M_w}{10^6 c_p T}$	(5)

Table 2: Input parameters used in the polymer bulk viscosity model. Second column indicates variable name used in the IORCoreSim manual.

	Name	Description	units
$M_{w0}$	MwO	Initial molecular weight	g/mol
$\alpha_{Mw}$	alfaMw	Exponent for dependency of $[\eta]$ om $M_w$	-
$T_0$	Tref	Reference temperature for temperature dependent $[\eta]$	°C
$B_{pT}$	Tfact	Temperature parameter for intrinsic viscosity $[\eta]$	1/°C
$[\eta]_0$	eta	Intrinsic viscosity $[\eta]$ for $M_{w0}$ at temperature $T_0$	ml/g
$k'$	hug1	Huggins constant, second polymer viscosity parameter	-
$k''$	hug2	Third polymer viscosity parameter	-
$a_n$	carr_na	1 <sup>st</sup> parameter for shear thinning exponent $n$	-
$b_n$	carr_nb	2 <sup>nd</sup> parameter for shear thinning exponent $n$	-
$\lambda_a$	carr_la	Parameter for the polymer relaxation time $\lambda_1$	kmol·K/J
$x_1$	carr_x1	Parameter defining the sharpness of the transition between Newtonian and shear thinning fluid.	

The specific viscosity used in Table 1, and plotted in Figure 1, is defined:

$$\eta_{sp} = \frac{\eta_p}{\eta_s} - 1, \quad (6)$$

where  $\eta_p$  and  $\eta_s$  are the viscosity of the polymer solution and the solvent, respectively.

The units for the input parameters are given in Table 2. Other units needed in the determination of these parameters are [g/ml] for the polymer concentration  $c_p$ , [cp] or [mPa·s] for viscosity in, and either [°C] in Eq. (1) or [K] in Eq.(5) for the temperature.

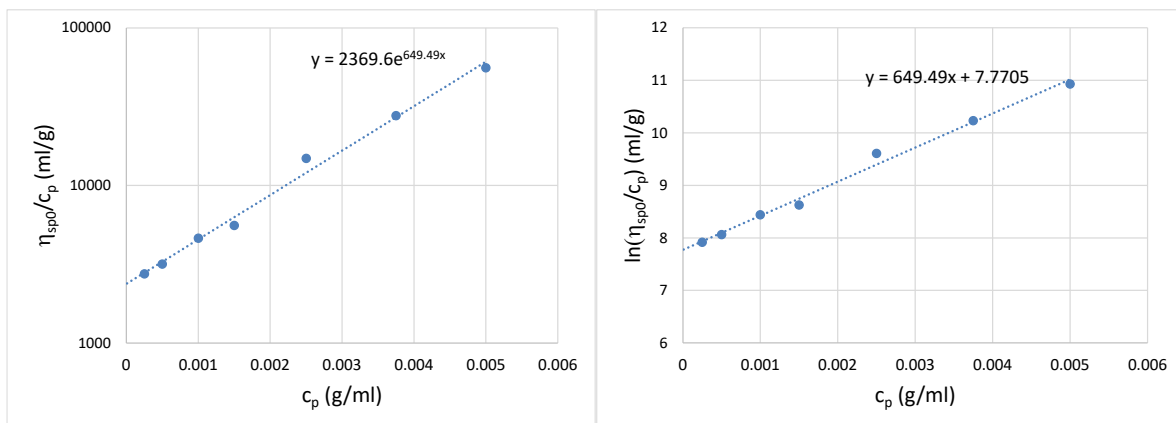


Figure 2: Determination of  $[\eta]$  and  $k'$  or HPAM (3530S,  $M_w$  15·10<sup>6</sup> g/mol, 30 % hydrolysis) from either exponential fit (left) or linear fit (right).  $[\eta]=2370$  ml/g and  $k'=0.274$ .

There are different methods for determining parameters. One option is to first determine  $[\eta]$ ,  $k'$  and optionally  $k''$  (if Eq. (2a) is used) from the variation of the Newtonian viscosity versus polymer concentration. Different techniques can be used to determine the intrinsic viscosity

as the limiting value of  $\eta_{sp}/c_p$  when  $c_p$  approaches zero. Using the Martin's Eq. (2a), a plot of  $\ln(\eta_{sp0}/c_p)$  versus  $c_p$  should form a straight line from which  $[\eta]$  and  $k'$  can be determined. An example of this is given in Figure 2.

The shear thinning index  $n$  and relaxation parameter  $\lambda_1$  can be determined from individual viscosity curves by the method indicated in Figure 1. Then the input parameters  $a_n$  and  $b_n$  can be obtained e.g. from rearranging Eq. (4) to get a linear plot of

$$\ln(n/(1-n)) = n_b \ln(n_a) + n_b \ln(c_p[\eta]).$$

The relaxation parameter  $\lambda_a$  can be obtained from a linear plot of  $\lambda_1$  versus  $\frac{\eta_s \eta_{sp0} M_w}{10^6 c_p T}$ . For the last parameter,  $x_1$  in Eq. (3), we only need an approximate value, normally using  $x_1 = 1$  will do, but cosmetic improvement can be obtained by matching this parameter as well.

An alternative to the method described above is to match all data at once, which is the method used for the data in Figure 3. First, the bulk viscosity model is coded in Excel (the equations in

Table 1) and linked to a set of initial values for the input parameters listed in Table 2. We use the model to calculate a viscosity for each experimental point. Then we use the Solver Add-ins in Excel to determine all relevant input parameters at once by minimizing the squared relative difference between measured and computed parameters for all the experimental points:

$$F = \sum_{i=1}^N w_i \left( \frac{\eta_{i,calc} - \eta_{i,m}}{\eta_{i,m}} \right)^2 \quad (7)$$

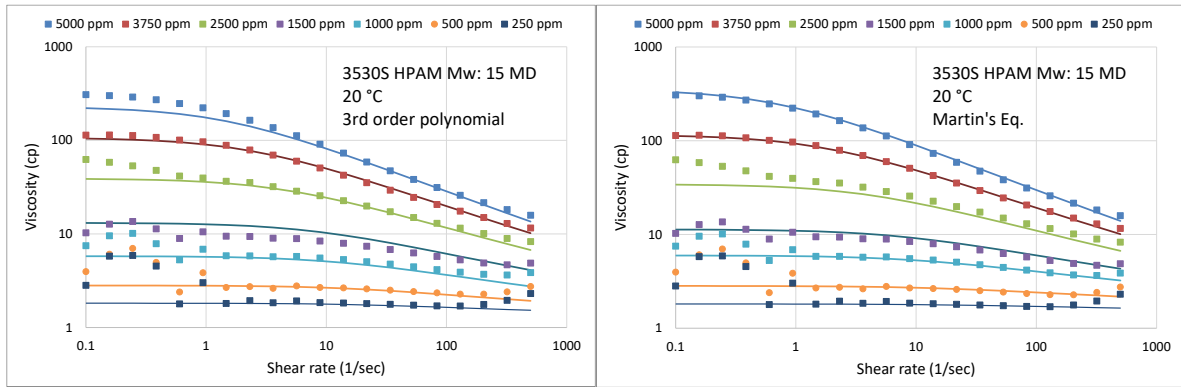


Figure 3: Viscosity profiles for HPAM (3530S,  $M_w$  15·10<sup>6</sup> g/mol, 30 % hydrolysis) at different concentrations in synthetic sea water at 20 °C. The zero rate  $\eta_{p0}$  is computed with Eq. (2a) in the left figure, and Eq. (2b) in the right figure.

The experimental data in Figure 3 shows significant scattering in measured viscosity at lower shear rates except for the series with higher polymer concentration. At the high shear rate end, a change towards increasing viscosity is observed for all series in the last 2-3 points. This is not a shear-thickening effects as observed for flow through a porous medium, but rather an effect of instability at high rotational speeds. The function  $w_i$  in Eq. (7) is included to remove this kind of noisy data from the parameter matching by using  $w_i=0$  for experimental outliers and  $w_i=1$  for good data.

Results from the matching of viscosity data in Figure 3 are presented in the form used in IORCoreSim input files in Input 1 and Input 2. The selected piece shows the relevant keyword in red (`cmpprop`), which triggers the reading of different polymer properties. The matched bulk

viscosity parameters (see Table 2 for a description) are represented with dark red values, while molecular weight and exponent  $\alpha_{Mw}$  obtained from other sources are in orange. The parameters in Input 1 are matched using the third order polynomial Eq. (2a) for the concentration dependency. Using Eq. (2b) instead gives in this case a slightly better overall match of the concentration dependency. The most important of the matched parameters is the intrinsic viscosity  $[\eta]$  because of its explicit use in sub-models handling in-situ polymer behavior. The difference in estimated  $[\eta]$  between Input 1 and Input 2 is only 3%. The parameters related to shear thinning show a larger change, partly in response to their direct dependency on  $[\eta]$  or  $\eta_{spo}$  (Eq. (4) and Eq.(5)) but also because they act as tuning parameters for the best overall viscosity match by compensating for any mismatch in the calculated  $\eta_{spo}$ .

The main effects of temperature on polymer solutions are that the viscosity scales approximately with the solvent viscosity and that the Newtonian plateau extends to a higher shear rate due to shorter relaxation times  $\lambda_1$  when molecules diffuse faster. The scaling of diffusion rate with temperature is included in Eq. (5) with the term  $\eta_s/T$ . These mechanisms are based on physical principles and need no additional input. Based on observations that  $[\eta]$  tends to decrease somewhat with increasing temperature, a simple empirical correction to  $[\eta]$  is added in Eq. (1). The temperature correction factor  $B_{pT}$  (*Tfact*) included in Input 1 and Input 2 is obtained for another polymer (Figure 4) of the same type, but with a higher molecular weight ( $18 \cdot 10^6$  Dalton).

#### Input 1: Bulk viscosity parameters for HPAM 3530S in sea water.

```

•hp1530 Mw=15 MDa, 30 %hydrolysis (3530S)
cmpprop
•Polymer
•name      Pref    Bf  density  compr  iads  vismodel
hp1530    1      1  1        0      almir  3 / almir = irreversible Langmuir Type
•eta      hug1    hug2  Tref    Tfact   Mw0    alfaMw
2424 0.247 0.091 20    0.0023 15000000 0.6 / viscosity at low shear
•Carr_na  Carr_nb Carr_la  Carr_le Carr_x
0.0782 0.560 0.00031 1.0    1.0 / shear thinning
•b        Qm      ScaleFlag (adsorption)
1000000  0.00046  1 /
•kref (mD)  pororef alfa
500      0.25    0.3 /
/

```

#### Input 2: Alternative viscosity parameters for HPAM 3530S in sea water using Martin's Eq. (2b).

```

•hp1530 Mw=15 MDa, 30 %hydrolysis (3530S)
cmpprop
•Polymer
•name      Pref    Bf  density  compr  iads  vismodel
hp1530    1      1  1        0      almir  3 / almir = irreversible Langmuir Type
•eta      hug1    hug2  Tref    Tfact   Mw0    alfaMw
2356 0.281 -1    20    0.0023 15000000 0.6 / viscosity at low shear
•Carr_na  Carr_nb Carr_la  Carr_le Carr_x
0.0874 0.834 0.00042 1.0    1.0 / shear thinning
•b        Qm      ScaleFlag (adsorption)
1000000  0.00046  1 /
•kref (mD)  pororef alfa
500      0.25    0.3 /
/

```

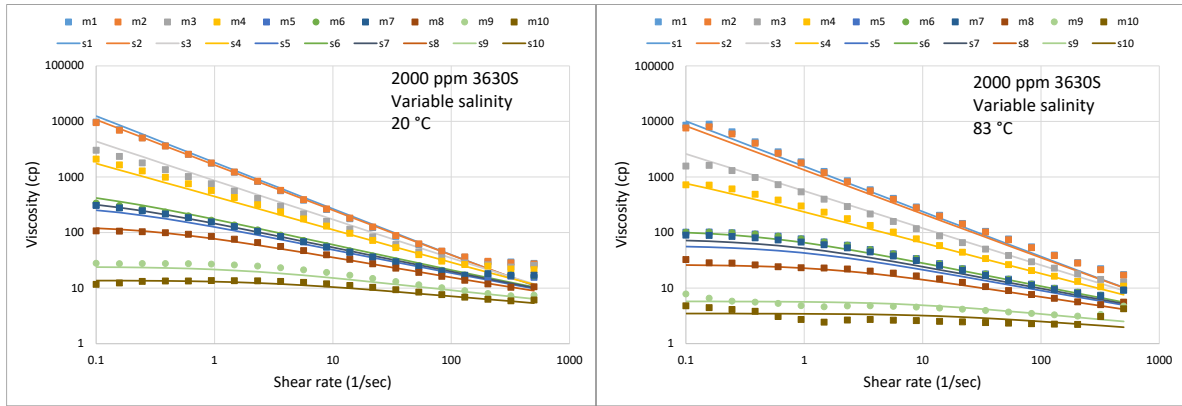


Figure 4: Viscosity profiles for 2000 ppm HPAM (3630S,  $M_w$   $18 \cdot 10^6$  g/mol, 30 % hydrolysis) dissolved in different brines at 20 °C (left) and 83 °C (right figure). Total salinity and Ca/Na ratio are varied. The lines representing the polymer model are computed from a single set of matched parameters used for both temperatures.  $B_{pT} = 0.0023$

Figure 4 demonstrates the large effect of salinity on HPAM polymers. The brines are made up by varying both the NaCl/CaCl<sub>2</sub> ratio and the total salinity from 20 to 10000 ppm. As can be seen, there is a large viscosity gain in using brines with reduced salinity if available. A full description of the salinity model can be found in the IORCoreSim manual. In short, an effective salinity computed from ions in solution is used to modify the intrinsic viscosity. The results in Figure 4 show that this rather simple model can give a good overall match of the viscosity with up to three order of magnitude variations at low shear rate. Furthermore, the model matches the measured data at two temperatures (20 and 83 °C) with the help from a single temperature correction factor  $B_{pT}$  ( $T_{fact}$ ). Being critical, one might see some room for improvement of the salinity model in handling the effect of varying the Na/Ca ratio.

### Flow in porous medium

To handle polymer flow in a porous medium, IORCoreSim make use of two components, one representing the volumetric concentration and a second component representing the molar concentration. In that way, the molecular weight can be tracked if mechanical or chemical degradation take place. The molar component requires no user actions but is generated automatically when a polymer component is defined, and injected molar concentrations are computed from the injected volumetric concentration and the initial molecular weight.

Equations describing the in-situ behavior of polymer is given in Table 3. Most of the equations describe physical relations with relatively few input parameters (in dark red color). The input parameters are listed with a brief description in Table 4. Most of the parameters are assumed to be reusable, i.e., that they can be used with a new polymer with little or no adjustments. Reusability is discussed more in the following sections.

Table 3: In-situ polymer equations in IORCoreSim. Input parameters in dark red.

Pore space available for the polymer, $E_{pv}$ :	$E_{pv} = S_w E_{pv0} E_{pva} E_{pvd}$ ,	(8)
Corrections for	$E_{pv0} = 1 - I_{pv0}$ , $E_{pva} = 1 - A_{pt}$ ,	
- inaccessible pore volume ( $I_{pv0}$ )		
- space occupied by adsorption ( $A_{pt}$ )	$E_{pvd} = 1 - \left(\frac{\delta}{R_{pw}}\right)^2$ , $\delta = f_{dpl} R_h$	
- depletion layer thickness ( $\delta$ )		
Hydraulic radius of pore space available for the polymer solution [ $\mu\text{m}$ ]:	$R_{pw} = 2.81 \sqrt{\frac{k k_{rw} \tau_w E_{pva}}{\phi S_w E_{pv0}}}$	(9)
Units: $k$ [D], $R_{pw}$ [ $\mu\text{m}$ ]		
Hydrodynamic radius of polymer in solution, $R_h$ [ $\mu\text{m}$ ], $M_w$ [g/mol], $[\eta]$ [ml/g]:	$R_h = 5.4 \cdot 10^{-5} (M_w [\eta])^{\frac{1}{3}}$	(10)
In-situ shear rate:	$\dot{\gamma} = \alpha_c \cdot \frac{4 u_w }{E_{pva} \sqrt{8 k k_{rw} \phi S_w E_{pv0} E_{pva}}}$ ,	(11)
Adsorption [PV fraction], Langmuir type:	$A_p = \frac{b c_p^w Q_m}{1 + b c_p^w}$	(12)
Effective water filled pore space fraction occupied by adsorbed polymer:	$A_{pt} = f_{mrp} \frac{A_p [\eta] \rho_p}{2.5 S_w E_{pv0}}$	(13a)
$f_{sh}$ includes an optional reduction in $A_{pt}$ at high shear rates. At low shear rate, $f_{sh} = 1$ .	$A_{pt} = f_{mrp} \frac{A_p}{S_w E_{pv0}} \left( (0.4 [\mu] \rho_p - 1) f_{sh} + 1 \right)$	(13b)
	$\lambda_3 = \frac{C_{rp}}{C_{el}} \cdot \lambda_2$ , $f_{sh} = (1 + (\lambda_3 \dot{\gamma})^{x_{rp}})^{-n_{rp}/x_{rp}}$	
Permeability reduction due to adsorbed polymer:	$RRF = \frac{1}{E_{pva}^2}$	(14)
Depletion layer thickness:	$\delta = \begin{cases} f_{dpl} R_h, & c_p^* \leq c_{p^*} \\ f_{dpl} R_h (c_p^*/c_{p^*})^{\alpha_{dp}}, & c_p^* > c_{p^*} \end{cases}$ ,	(15)
	$c_{p^*} = \frac{1}{f_{cpdo} [\mu]} \cdot c_p^* = \frac{c_p}{E_{pv0} E_{pva}}$	
Optional, polymer partitioning between depletion layer ( $c_{pd}$ ) and bulk polymer phase ( $c_{pp}$ ):	$R_{cpd} = \frac{c_{pd}}{c_{pp}}$	(16)
Apparent viscosity:	$\eta_{pa} = \frac{\eta_{pb}}{M_v - (M_v - 1) E_{pvd}^2}$ , $M_v = \frac{\eta_{pb}}{\eta_{dpl}}$	(17)
Viscosity: $\eta_{pb}$ : bulk, $\eta_{dpl}$ : depletion layer		
Onset of elongational flow [s]:	$\lambda_2 = C_{el} \cdot 3.61 \cdot 10^{-11} \sqrt{\frac{k_{rw} E_{pva}}{S_w}} \cdot \frac{\phi \eta_s [\eta] M_w}{(1 - \phi) T}$	(18)
Units: $\eta$ : [mPa·s], $[\eta]$ : [ml/g], $M_w$ : [g/mol]		
Effective in-situ viscosity:	$\eta_p = (\eta_{pa} - \eta_s) (1 + (\lambda_2 \dot{\gamma})^{x_2})^{(m+n)/x_2} + \eta_s$	(19)
Mechanical degradation at high shear rates:	$\frac{dM_w}{dt} = -k M_w^2$ , $k = \frac{2(r_d \eta_p \dot{\gamma})^{\alpha_d}}{10^6 \cdot R_{pw}}$	(20)
Units: $\eta_p$ [Pa·s], $M_w$ [g/mol], $R_{pw}$ [ $\mu\text{m}$ ], $\dot{\gamma}$ [ $\text{s}^{-1}$ ] and $t$ [s].		
Tortuosity, improved representation of variations in porosity and saturation:	$\tau_w = \phi^{1-m} S_w^{1-n_w}$	(21)

Table 4: Input parameters related to in-situ behavior of polymer. Second column indicates variable names used in the IORCoreSim manual. Dependency on polymer type and salinity indicated by color; blue: independent, dark red; highly dependent, black (the rest) little or no dependency.

	Name	Description
$\alpha_c$	alfac	In-situ shear rate parameter
IPVO	IPVO	Fraction microporosity inaccessible for polymer
Depletion layer		
$f_{dpl}$	fdpl	Multiplication factor for thickness of depletion layer, $\delta = f_{dpl} \cdot R_h$ .
$R_{cpd}$	Rcpd	Ratio of polymer in depletion layer (default=0)
$\alpha_{dp}$	alfadpl	Exponent for concentration dependent depletion layer (default=0)
$f_{cpd0}$	fcpd0	Depletion layer thickness is constant for $c_p$ below $c_{p^*}=1/fcpd \cdot [\eta]$
Permeability reduction ( <i>RRF</i> )		
$f_{mrp}$	fmrp	Tuning factor for permeability reduction
$C_{rp}$	rp_lamf	Parameter for onset of reduced <i>RRF</i> at higher shear rates
$n_{rp}$	rp_n	Exponent for reduced <i>RRF</i>
$x_{rp}$	rp_x	Sharpness parameter for transition to reduced <i>RRF</i>
$S_{0p}$	Sop	Specific surface area of polymer in [m <sup>2</sup> /ml], (default=7000)
Elongational flow		
$C_{el}$	el_lamf	Tuning parameter for relaxation time $\lambda_2$ defining onset of elongational flow.
$m$	el_m	Shear thickening index.
$x_2$	el_x2	Parameter $x_2$ for the transition between shear thinning and shear thickening.
$r_d$	degr_ratef	Degradation rate factor, $r_{deg}$ . Units: see Eq. (20)
$\alpha_d$	degr_alfa	Degradation exponent (default=3)
Tortuosity		
$m$	m	Rock cementation index (from electrical resistivity at 100% $S_w$ )
$n_w$	nw	Saturation index (from resistivity versus $S_w$ )

### Single phase core experiments

The model parameters handling in-situ behavior of polymer can be determined from single-phase (100% water saturated) core floods of the type shown in Figure 5. The flowrate should be varied to cover the shear rate variations expected in a reservoir. The results in Figure 5 for a hydrolyzed polyacrylamide show three distinct flow regimes; shear thinning behavior at low rate, shear thickening behavior at intermediate rate and shear degradation at high flow rates. In addition to the results in Figure 5, one would need *RRF* after displacing the polymer solution out of the core and preferentially the effluent polymer viscosity from the shear degradation regime. Here we present results typical for synthetic polymers, however the same type of experiments should be used to match relevant models for biopolymers.

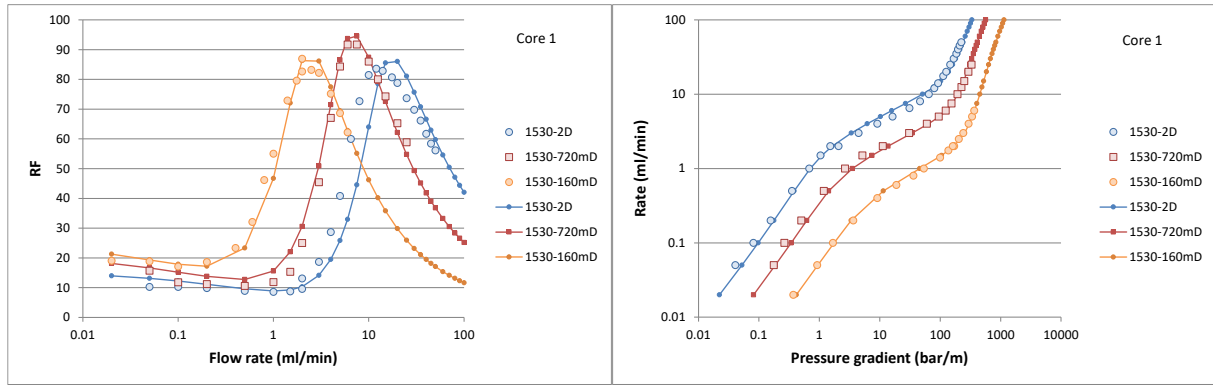


Figure 5: Multirate results with 1500 ppm HPAM (3530S,  $M_w$   $15 \cdot 10^6$  g/mol, 30 % hydrolysis) dissolved in synthetic seawater at 20 °C flooded through core plugs with different permeability, experimental (markers) and simulated (lines) with parameters from Input 1 and Input 3. Core diameter is 3.8 cm.

The task of the model is to link flow rate with bulk viscosity and  $RRF$  so that observed pressure gradient is reproduced. The first thing needed for that is the in-situ shear rate. The in-situ shear rate expression in Eq. (11) is derived using a capillary tube approach with  $\alpha_c$  as a pre-factor accounting partly for properties of the formation (e.g., averaging pore size distribution) and that we don't want the correct surface shear rate, but rather an effective shear rate that links to an apparent polymer bulk viscosity which we can apply in a Newtonian model. We assume that with the expression used in Eq. (11),  $\alpha_c$  should not vary much for different formations. An indication of that is the good match of the onset of elongational flow obtained for different permeabilities using a constant  $\alpha_c$ . If  $\alpha_c$  is increased with a factor, then the elongation parameter  $C_{el}$  must be decreased with the same factor to get a similar match (other parameters may be affected as well).

The parameters matched to data in Figure 5 are given in Input 3. In addition, core experiments with three other polymers of the same type, but with  $M_w$  ranging from 5 to 20 MDalton, were included in the determination of these parameters. A matching procedure starting from scratch can be described by the steps:

1. Assign an appropriate value to the in-situ shear rate parameter, e.g.,  $\alpha_c=2$ .
2. Assign a value for the fraction of the pore space with micropores inaccessible for polymer, e.g., the fraction with radius less than 0.1  $\mu\text{m}$  from a pore size distribution. Here we used  $IPVO=0.1$  for most of the cores. The  $IPVO$  affects the polymer transport velocity, but the effect is normally much smaller than the effect of the depletion layer [5] and an approximate value is fine.
3. Determine adsorption and parameter  $f_{mrrp}$  so that experimental  $RRF$  is matched. This is described in the next section.
4. Assign depletion layer parameters to match  $\Delta p$  at the low flow rate end. For the cases in Figure 5, the simplest model with constant depletion layer thickness equal to  $R_h$  was sufficient. Thus, a single input parameter  $f_{dpl}=1$  was used.
5. Determine elongational parameters  $C_{el}$ ,  $m$  and  $x_2$  by matching the shear thickening regime.
6. Determine the degradation rate constant  $r_d$  and exponent  $a_d$  by matching the declining  $\Delta p$  at the high flow rate end.
7. Compare measured effluent viscosity with viscosity calculated from simulated  $M_w$  of produced polymer. The effluent viscosity can be matched by introducing a shear dependent reduction in  $RRF$  (parameters  $C_{rp}$ ,  $n_{rp}$  and  $x_{rp}$ ). Produced  $M_w$  and effluent viscosity will also depend on the Mark Houwink exponent  $\alpha_{Mw}$  in Eq. (1).
8. Introducing a shear rate dependent  $RRF$  requires a retuning of the degradation and possibly the depletion layers parameters.

If matched to a single experiment, one should be aware that the solution is non-unique, i.e., that different combinations of parameters can produce a similar match. If matched to several experiments, the parameters become more general, and the model can be used for reliable predictions within the variable space covered by the experiments. The parameters in Input 3 can be used to predict behavior of HPAM dissolved in sea water in different formations, but since all the experiments were done with the same concentration 1500 ppm (one exception with 600 ppm), the model would not be reliable at much higher concentrations.

Figure 7 shows that the Input 3 parameters fail at higher polymer concentrations with predicted (simulated)  $RF$  at low shear rate levelling off at a plateau value below 30. Including concentration dependency in the depletion layer (Input 4) produces an increasing  $RF$  more in line with results published by Howe, et al. [5]. The match with the 1500 ppm case is preserved with the second parameter set. This indicates that it should be possible to get a more general depletion layer model by including experiments at higher concentrations in the dataset used for matching. Further testing against experimental data may also reveal shortcomings of the model, like eventual dependency of shear rate and salinity.

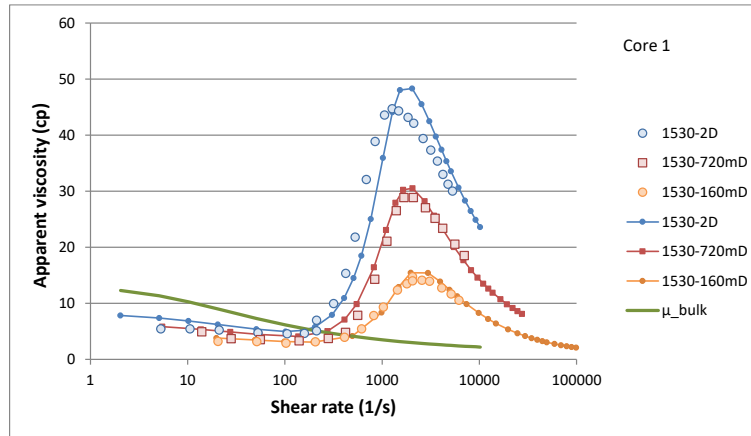


Figure 6: Apparent viscosity results with 1500 ppm HPAM 3530S, computed from experimental and simulated results in Figure 5 and plotted versus in-situ shear rate. Green line indicates the corresponding bulk viscosity.

If another polymer type is tested or if the salinity is reduced, we would expect that most of the parameters could be reused as indicated by the color code in Table 4. The dependency on polymer properties for the depletion layer thickness, the onset of elongational flow and the  $RRF$  is included in these models by using information obtained from the bulk viscosity input. The parameters  $m$ ,  $x_2$  and  $r_d$  used in the shear thickening response and degradation rate equations differs from the other parameters in that they are explicitly representing some polymer property which we (at present) cannot predict. So, with a new polymer, these three parameters must be determined, while the rest can be reused or only require some fine tuning.

When comparing experimental and simulated result:

- Initial rate when polymer is first injected into the core must be the same as in the experiment. If mechanical degradation take place, there will be a  $M_w$  gradient for adsorbed polymer throughout the core and consequently a gradient in  $RRF$ .
- Experimental and simulated  $\Delta p$  for each rate can be compared directly, while properties like  $RF$  and shear rate should be computed from the simulated results in the same way as for the experimental data. This is due to in-situ gradients of these properties that will appear in the shear degradation regime and due to eventual gradients in  $RRF$ .
- The adsorption should be set to irreversible to secure that correct  $RRF$  is computed from simulated  $\Delta p$  after the post water flood.

Input 3: Parameter set for HPAM in sea water.

```

rockshear
•alfac
 2.0 /
polyIPV :inaccessible pore volume
•IPV0 dplFlag fdpl aM tau Rcpd alfadp fcpd0
 0.1 2 1. /
polyrkf : RRF model
*fmrp rp_mod rp_lamf rp_n rp_x S0p
 1.0 3 0.5 1.0 4 7000. /
polydegr : shear thickening and mechanical degradation
•el_lamf el_m2 el_x2 degr_ratef degr_alfa degr_beta
 4.0 1.5 3.0 0.0015 3.0 /
rtort : Rock tortuosity using Archie's resistivity model tau=tau(porosity,Sw)
•m nw
 1.7 2. /

```

Input 4: Alternative parameter set with improved concentration dependency:

```

rockshear
•alfac
 2.0 /
polyIPV :inaccessible pore volume
•IPV0 dplFlag fdpl aM tau Rcpd alfadp fcpd0
 0.1 2 1.4 1.3 0.1 -0.4 0.3 /
polyrkf : RRF model
*fmrp rp_mod rp_lamf rp_n rp_x S0p
 1.0 3 0.2 1.0 2 7000. /
polydegr : shear thickening and mechanical degradation
•el_lamf el_m2 el_x2 degr_ratef degr_alfa degr_beta
 4.0 1.5 3.0 0.0015 3.0 /
rtort : Rock tortuosity using Archie's resistivity model tau=tau(porosity,Sw)
•m nw
 1.7 2. /

```

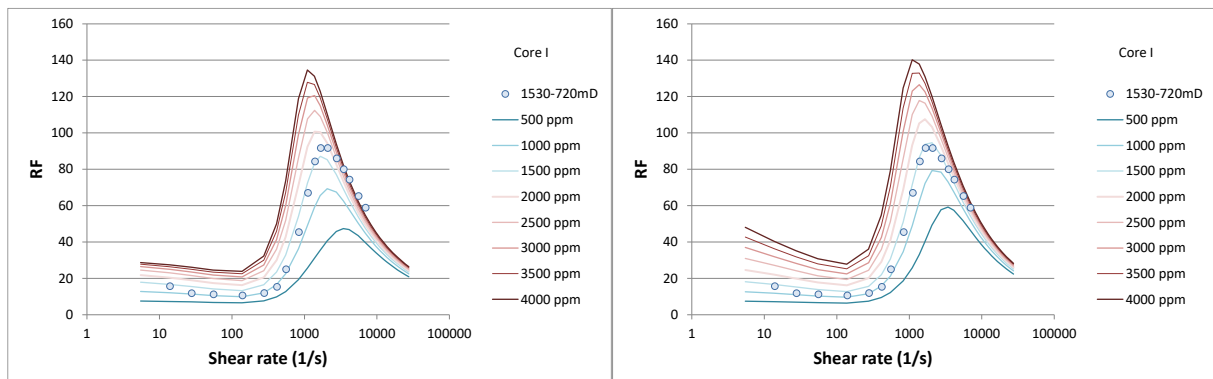


Figure 7: Effect of concentration, HPAM 3530S in synthetic seawater. Simulated with model parameters from Input 3 (left) and Input 4 (right). Markers indicate experimental results for the 1500 ppm case.

### Adsorption and permeability reduction

Polymer retention can be due to adsorption on the pore surface and mechanical trapping of polymer molecules in narrow parts of the pore space. Only the first mechanism is implemented in IORCoreSim. Polymer exhibiting mechanical trapping will gradually block the porous medium as more polymer is injected and is thus not candidates for in-depth polymer flooding of a field. Furthermore, polymer solutions are polydisperse and simulating trapping with a monodisperse model will result in an erroneous length effect. A proper modeling of mechanical trapping could be done by splitting the  $M_w$  distribution into several sub-components and relate the probability for being trapped to  $M_w$  along the lines done in Lohne, et al. [6].

The adsorption in IORCoreSim is in units pore volume (PV) fraction. The available adsorption models are of the Langmuir type or tabular format (free format), both in kinetic and equilibrium versions, and with the possibility to include dependency on core properties, temperature, salinity and the presence of other species. The choice of model would depend on the purpose of the simulation. For the matching of steady-state results like that in Figure 1, an irreversible Langmuir type option is recommended. In a field case situation, it could be important to use a reversible adsorption model that capture the slow decline in  $RRF$  during the post polymer water injection.

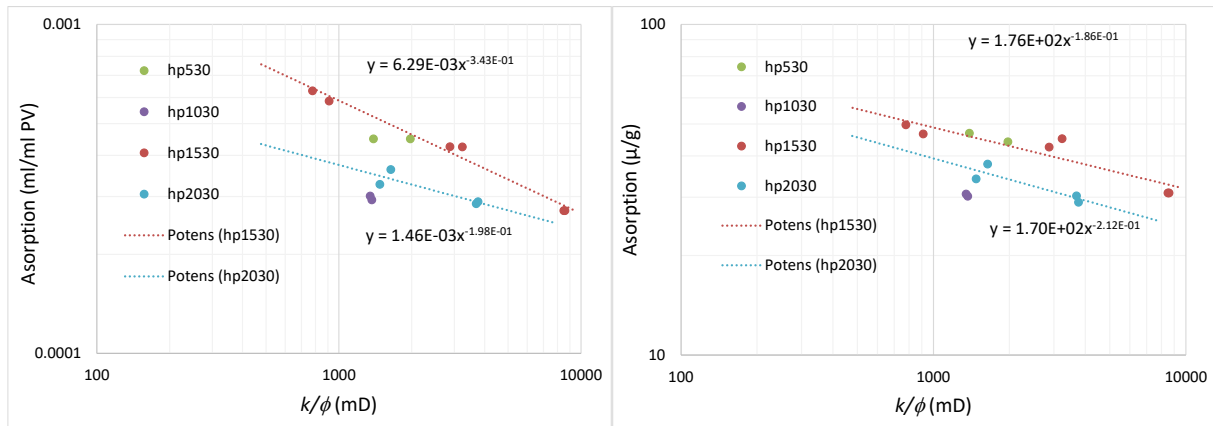


Figure 8: HPAM adsorption estimated from  $RRF$  in outcrop cores. Plotted as PV fraction (left) and  $\mu\text{g/g}$  (right).

The adsorption is linked to the measured  $RRF$  using Eq. (13a) which determines the tuning parameter  $f_{mnp}$ . Alternatively,  $f_{mnp}$  can be determined by matching  $RRF$  in the simulations. In the HPAM cases presented here, the actual adsorption was not measured but instead estimated from the matching of  $RRF$  using  $f_{mnp}=1$ . The resulting adsorption values are plotted in Figure 8 versus  $k/\phi$  and indicates a proportionality close to  $(k/\phi)^{-0.3}$ . These values are for outcrop core material. For evaluation of implementation in a field, adsorption and  $RRF$  should be measured on reservoir material under representative wettability conditions.

### Two-phase experiments

Two-phase experiments should be available to ensure that the model derived from single-phase experiments is able to handle the presence of oil. For field evaluation purposes, it will also be valuable to do such experiments at relevant wetting conditions. A challenge is to perform such experiments in a way so that  $RF$  values can be extracted. A method could be to first waterflood the core with several pore volumes, re-establish  $S_{wi}$  and then inject e.g., 0.5 PV water followed by a polymer solution, and then do some rate variations when the oil production ceases. The rate should be kept low (reservoir rate) not entering the shear thickening regime before at the end. Relative permeability functions derived from the first waterflood is used as input in the second flood to evaluate the polymer effect.

### Recommended workflow

The model parameters presented in this report (Input 3 or Input 4) are valid for 1500 ppm HPAM (30% hydrolysis degree) dissolved in sea water. If the salinity is changed, a higher polymer concentration is used or if another polymer is used, then the model parameters must be tuned. Several parameters may be reused as indicated in Table 4. The proposed steps in matching a new polymer are summarised in Table 5.

Table 5: Polymer workflow – for matching IORCoreSim polymer model to a new polymer

Experimental	IORCoreSim
<b>Bulk viscosity</b>	Parameters in Table 2 (Input 1)
<ul style="list-style-type: none"> <li>Effects of shear rate, concentration and temperature</li> </ul>	Match parameters. Equations for bulk viscosity are given in Table 1.
<b>Single-phase core flood(s)</b>	Parameters in Table 4
Measured	Equations for in-situ polymer behavior are given in Table 1.
<ul style="list-style-type: none"> <li><math>\Delta p</math> versus flow rate</li> <li>Effluent viscosity (if degradation)</li> <li><math>RRF</math></li> </ul>	<ul style="list-style-type: none"> <li>Start with values given in Input 3 or Input 4.</li> <li>If adsorption is measured, tune <math>f_{mrp}</math> to match <math>RRF</math>, or else estimate adsorption from <math>RRF</math> using <math>f_{mrp}=1</math>.</li> </ul>
One core flood is sufficient for a first evaluation of a polymer.	If viscosity ratio $\eta_{p0}/\eta_s > 25$ :
	Match $\Delta p$ at low and intermediate shear rate:
	<ul style="list-style-type: none"> <li>Adjust depletion layer parameters</li> <li>May have to tune rate dependency of <math>RRF</math> (<math>C_{rp}</math>, <math>n_{rp}</math> and <math>x_{rp}</math>)</li> </ul>
	<b>Elongational flow</b>
If there are significant changes in model parameters, additional core floods is recommended.	Match $\Delta p$ at high shear rate and effluent viscosity by tuning:
	<ul style="list-style-type: none"> <li>Shear thickening parameters <math>m</math> and <math>x_2</math></li> <li>Degradation rate factor <math>r_d</math></li> <li>Rate dependency of <math>RRF</math> (<math>C_{rp}</math>, <math>n_{rp}</math> and <math>x_{rp}</math>)</li> </ul>
<b>Two-phase experiment</b>	<b>Validation of model</b>
	To ensure that the model derived from single-phase experiment can handle the presence of oil.

## Validation

The validation of the proposed method lies in the comparison with experimental data. The recommended polymer model matched to a series of core experiments conducted with HPAM in sea water, is shown to replicate observed results at different permeabilities and with different molecular weights using a single set of input parameters for the in-situ rheological behavior. The bulk viscosity model has been shown to replicate experimental shear thinning viscosity at varying polymer concentrations, temperatures, and salinity.

The model is considered validated for predicting polymer behavior within the variable space covered in the experimental data base used for determination of model parameters. If one wants the model to predict polymer flooding at conditions not covered, i.e., with higher polymer concentrations and at different temperatures, then additional experiments would be needed for validation and adjustment of the model parameters.

## Conclusions and recommendations

The proposed tool for interpretation and extraction of model parameters from laboratory polymer experiments can reproduce experimental data at various conditions with a single set of model parameters. The model handles variations in permeability, temperature, polymer concentration and salinity. Once calibrated against sufficient laboratory experiments, it can be used as a predictive tool. The model is highly reusable, meaning that reliable predictions can be made for new polymers with less experimental input. The IORCoreSim simulator is not able to handle large field models, but it can be used to investigate behavior of polymer in small large-scale models. It can be used for evaluation of polymer injectivity including eventual

effects of shear thickening and mechanical degradation and to study polymer flow in heterogeneous formations.

Calibrating IORCoreSim to data and using IORCoreSim to predict new results, and test them in the lab will reduce the uncertainty in upscaling experimental polymer results from the laboratory to the field. More robust decisions can be made on implementing polymer flooding in a field. This approach has itself no direct environmental impact but may influence the probability for polymer being used. Polymer flooding has a potential for reduced CO<sub>2</sub> emission per unit oil produced due to less water being produced and injected. Dupuis, et al. [7] report that polymer flooding can reduce the CO<sub>2</sub>-emmission by 40-80% compared to a water flood per volume of oil produced.

### Knowledge Gaps

The outcome of the proposed recommended practice is a history matched polymer model which can be used for predictive simulations at varying conditions. At present, the method has only been validated against experimental data from the laboratory. A next major step will be to apply the results on field case data. The IORCoreSim simulator may be used directly for investigation of polymer injectivity and polymer pilots performed in a limited part of a reservoir. The IORCoreSim has however, limited reservoir description and is not able to handle larger models.

There is an ongoing activity on adding polymer functionality into Eclipse (using IORSim), OPM and Intersect (using Phyton scripts). An alternative method being looked into is using IORCoreSim to generate polymer input which can be used in e.g. Eclipse.

There are some additional uncertainties which should be solved regarding injectivity and the large grid block size used in field models.

The polymer injectivity is solved in IORCoreSim for a radial well penetrating a homogeneous well block. How will the rheological behavior of polymer flow through a smooth radial surface compare with the flow in a well with a certain perforation density? The injectivity may also be influenced by thermo and pressure induced fracturing.

There are two potential problems related to large grid blocks used in field models. The first is related to sub-grid heterogeneities and how the use of averaged block properties (permeability and porosity) may affect the polymer model. The second potential problem is increased numerical dispersion.

### References

1. Lohne, A., Nødland, O., Stavland, A., and Hiorth, A., "A model for non-Newtonian flow in porous media at different flow regimes," *Computational Geosciences*, vol. 21 (December), 2017.
2. Stavland, A., Jonsbråten, H.C., Lohne, A., Moen, A., and Giske, N.H., "Polymer Flooding – Flow Properties in Porous Media Versus Rheological Parameters," SPE 131103-MS presented at SPE EUROPEC/EAGE Annual Conference and Exhibition, Barcelona, Spain, 14-17 June 2010.
3. Jouenne, S. and Levache, B., "Universal viscosifying behavior of acrylamide-based polymers used in enhanced oil recovery," *Journal of Rheology*, vol. 64 (5), pp. 1295-1313, 2020.

4. Lohne, A., Stavland, A., and Reichenbach-Klinke, R., "Modeling of Associative Polymer Flow in Porous Medium," Tu B 08 presented at IOR 2019 - 20<sup>th</sup> European Symposium on Improved Oil Recovery, Pau, France, 8-11 April 2019.
5. Chauveteau, G., "Fundamental Criteria in Polymer Flow Through Porous Media," in Water-Soluble Polymers, *Adv. in Chem. Ser.*, J. E. Glass, Ed., 1986.
6. Howe, A.M., Clarke, A., and Giernalczyk, D., "Flow of concentrated viscoelastic polymer solutions in porous media: effect of Mw and concentration on elastic turbulence onset in various geometries," *Soft Matter*, vol. 11 (32), pp. 6419-6431, 2015.
7. Lohne, A., Han, L., van der Zwaag, C., van Velzen, H., Mathisen, A.-M., Twynam, A., Hendriks, W., Bulgachev, R., and Hatzignatiou, D.G., "Formation Damage and Well Productivity Simulation," *SPE Journal*, vol. 15 (3), pp. 751-769, 2010.
8. Dupuis, G., Al-Khoury, P., Nieuwerf, J., and Favero, C., "Using Polymer EOR to Reduce Carbon Intensity While Increasing Oil Recovery," IOR 2021, 2021.

Nomenclature	Greek symbols
$A_p$ : polymer adsorption (PV fraction)	$\alpha_c$ : in-situ shear rate constant
$A_{pt}$ : effective PV fraction occupied by $A_p$	$\delta$ : depletion layer thickness
$c_p$ : polymer concentration	$\dot{\gamma}$ : shear rate ( $s^{-1}$ )
$c_p^w$ : polymer water phase concentration	$\eta$ : viscosity
$E_{pv}$ : effective PV fraction available for polymer	$\lambda_n$ : relaxation parameter for polymer indicating onset of shear thinning ( $n=1$ ), elongational flow ( $n=2$ ) and reduced $RRF$ ( $n=3$ )
$k$ : permeability	$\rho$ : density
$K$ : Kelvin	$\tau_w$ : tortuosity for the water phase
$M_v$ : viscosity ratio (polymer/brine)	$\phi$ : porosity
$M_w$ : molecular weight	
$n$ : shear thinning index	Subscripts:
$PV$ : pore volume	$o$ : initial, reference value
$R_h$ : hydrodynamic radius of polymer	$a$ : apparent
$R_{pw}$ : hydraulic radius for polymer solution	$b$ : bulk solution
$RF$ : resistance factor	$p$ : polymer
$RRF$ : residual resistance factor due to $A_p$	$s$ : solvent
$S$ : saturation	$w$ : water phase
$t$ : time	
$T$ : temperature	